

# Bow shocks, bow waves, and dust waves. V. No dust wave for $\sigma$ Ori

William J. Henney & S. Jane Arthur

*Instituto de Radioastronomía y Astrofísica, Universidad Nacional Autónoma de México, Apartado Postal 3-72, 58090 Morelia, Michoacán, México*

Accepted XXX. Received YYY; in original form ZZZ

## ABSTRACT

We critically evaluate the role of radiation and ram pressure in providing internal support for the bow-shaped infrared arc around the massive triple star system  $\sigma$  Ori Aa/Ab/B in the IC434 H II region. We present evidence for hydrogen recombination line emission from the arc, which demonstrates that it cannot be a decoupled dust wave, as has previously been claimed. On the other hand, we show that the fraction of the stellar luminosity trapped by the arc is insufficient for it to be supported by radiation if the grains and gas are well coupled. Therefore, the arc must be supported by the ram pressure of an internal wind. However, the stellar winds from the OB stars in the  $\sigma$  Ori Aa/Ab/B system seem too weak to provide this support on their own. We propose instead that it is the photoevaporated disk wind from the enclosed proplyd IRS 1B that dominates the ram pressure support for the bow.

**Key words:** circumstellar matter – radiation: dynamics – stars: winds, outflows

## 1 WHY THE INNER ARC CANNOT BE A DECOUPLED DUST WAVE

We downloaded optical images of  $\sigma$  Ori from the Astronomical Data Centre of the Cambridge Astronomy Survey Unit.<sup>1</sup> These were obtained on 2008-11-19 with the Wide Field Camera of the Isaac Newton Telescope from an observational program of Rafael Barrena. We use images in two filters: a narrow-band H $\alpha$  filter (central wavelength,  $\lambda_0 = 656.8$  nm, full-width half maximum,  $\Delta\lambda = 9.5$  nm) and a broad-band Sloan Gunn  $R$  filter ( $\lambda_0 = 624.0$  nm,  $\Delta\lambda = 134.7$  nm). We have removed the bias v

## 2 WHY THE INNER ARC CANNOT BE RADIATION-SUPPORTED

SEDs of the two arcs

## 3 WEAK STELLAR WINDS FROM THE MASSIVE TRIPLE AA/AB/B

## 4 PHOTOEVAPORATION FLOW FROM THE PROPLYD IRS 1B

## 5 THE NATURE OF THE OUTER DUST ARC

## 6 CONCLUSIONS

## ACKNOWLEDGEMENTS

We are grateful for financial support provided by Dirección General de Asuntos del Personal Académico, Universidad Nacional

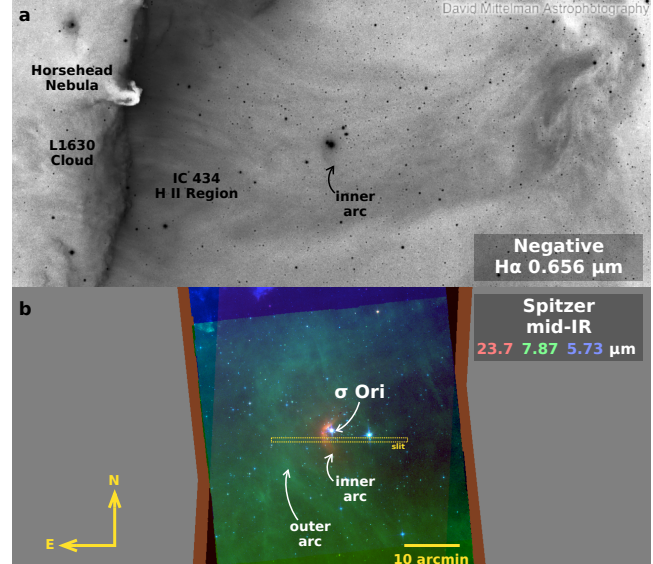


**Figure 1.** Optical and infrared images of  $\sigma$  Ori and its surroundings. (a) Optical image in the H $\alpha$  line, shown in negative grayscale. (b) Mid-infrared image in three Spitzer bands: MIPS 23.7  $\mu$ m (red), IRAC 7.87  $\mu$ m (green), and IRAC 5.73  $\mu$ m (blue). The yellow dashed box shows the slit for which profiles are extracted in Fig. 2.

Autónoma de México, through grant Programa de Apoyo a Proyectos de Investigación e Innovación Tecnológica IN107019. We thank Bo Reipurth for advice on astronomical data archives. This work is based in part on observations made in the Observatorios de Canarias del IAC with the Isaac Newton Telescope operated on the

<sup>1</sup> <http://casu.ast.cam.ac.uk/surveys-projects/adc>

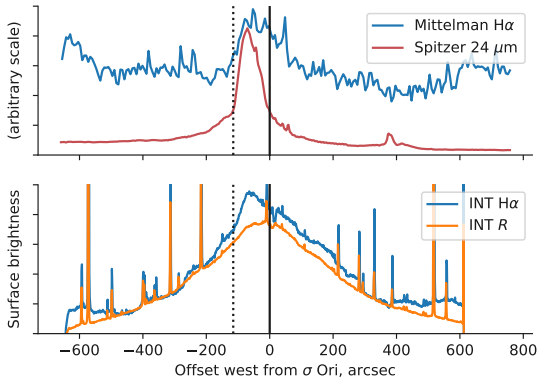


**Figure 2.** Brightness profiles through  $\sigma$  Ori inner arc. (a) H $\alpha$  and All profiles are extracted in a 40'' wide slit, offset by 80'' to the south of  $\sigma$  Ori, as indicated in Fig. 1b.

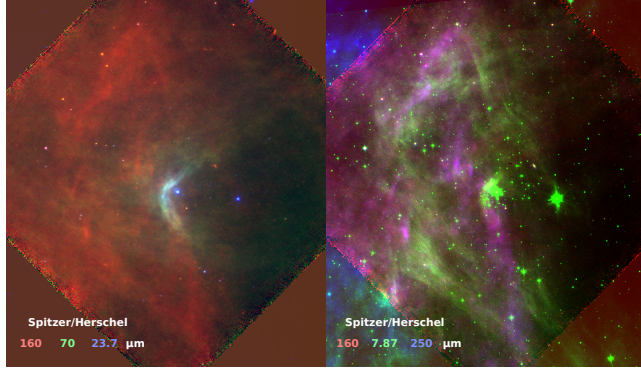


**Figure 3.** Combined mid-infrared and far-infrared views of the inner and outer arcs around  $\sigma$  Ori

**Figure 4.** Spectral energy distributions of arcs around  $\sigma$  Ori

island of La Palma by the Instituto de Astrofísica de Canarias in the Observatorio del Roque de los Muchachos. This work is based in part on observations made with the Spitzer Space Telescope, which is operated by the Jet Propulsion Laboratory, California Institute of Technology under a contract with NASA. This work makes use of imagery from David Mittelman Astrophotography.

## REFERENCES

This paper has been typeset from a Te<sub>X</sub>/L<sub>A</sub>T<sub>E</sub>X file prepared by the author.

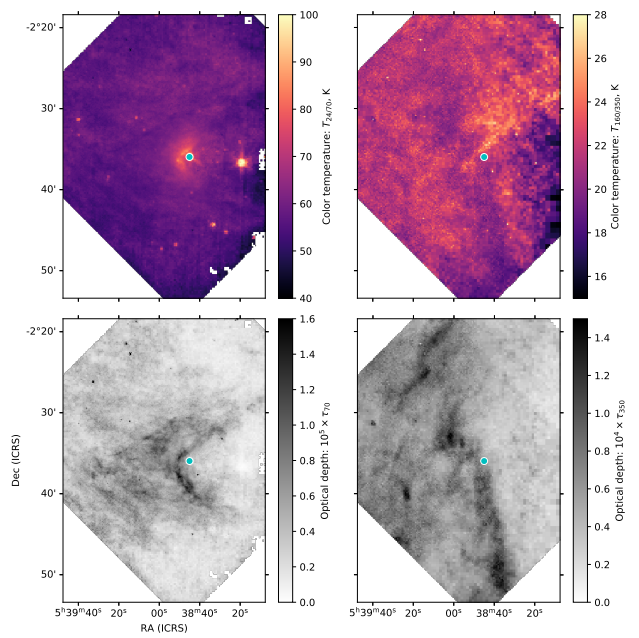


**Figure 5.** Maps of dust temperature and optical depth. (a) Color temperature derived from 24  $\mu\text{m}$ /70  $\mu\text{m}$ . (b) Color temperature derived from 160  $\mu\text{m}$ /350  $\mu\text{m}$ . (c) 70  $\mu\text{m}$  optical depth of warm dust component. (d) 350  $\mu\text{m}$  optical depth of cool dust component.

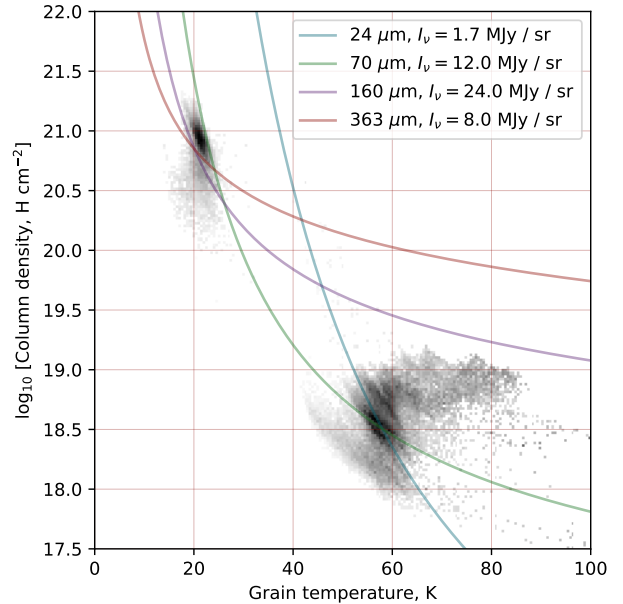


**Figure 6.** Joint distribution of dust temperature and gas column density. Gray-scale image shows the fraction of the emission at 160  $\mu\text{m}$  (cool component, upper-left) and 24  $\mu\text{m}$  (warm component, lower right) that is contributed by pixels with a given ( $T, N$ ) combination. Conversion from dust optical depth to hydrogen column density is carried out using the empirical calibration described in the text.